

Oriental Medicine

Active compounds in RenShenJian decoction ameliorate insulin resistance in vitro

Zhen-Hua Lan^{1,2#}, Lan-Fang Tan^{1,2#}, Guo-En Wang^{1,2#}, Meng-Qiu Tang^{1,2}, Ruo-Hong Wang^{1,2}, Shu-Mei Wang^{1,2*}

¹Guangdong Pharmaceutical University, Guangzhou 510006, China. ²Key Laboratory of Digital Quality Evaluation of Chinese Materia Medica of State Administration of Traditional Chinese Medicine and Engineering & Technology Research Center for Chinese Materia Medica Quality of Guangdong Province, Guangdong Pharmaceutical University, Guangzhou 510006, China.

[#]Zhen-Hua Lan, Lan-Fang Tan and Guo-En Wang contributed equally to this work.

*Corresponding to: Shu-Mei Wang. School of Pharmacy, Guangdong Pharmaceutical University, No. 280, East Ring Road, Guangzhou Higher Education Mega Center, Guangzhou 510006, China. E-mail: gdpuwsn@126.com.

Author contributions

Zhen-Hua Lan: investigation, validation, writing-original draft; Lan-Fang Tan: investigation, formal analysis, data curation; Guo-En Wang: supervision, writing-review & editing; Meng-Qiu Tang: data curation; Ruo-Hong Wang: visualization; Shu-Mei Wang: conceptualization, methodology, project administration.

Competing interests

The authors declare no conflicts of interest.

Acknowledgments

This work was supported by grants from National Natural Science Foundation of China (81773884), and National Science and Technology Major Project (2017ZX09301077), and Administration of Traditional Chinese Medicine of Guangdong Province (No. 20201195), and Guangdong Medical Science Foundation (No. B20191067). Technology funds were obtained from the Key Unit of Chinese Medicine Digitalization Quality Evaluation of State Administration of Traditional Chinese Medicine. We thank Editage Ltd. for editing the English text of a draft of this manuscript.

Abbreviations

RSJ, RenShenJian; GLUT4, glucose transporter isoform 4; AMPK, adenosine 5'-monophosphate-activated protein kinase; 2-NBDG, 2-(N-(7-nitrobenz-2-oxa-1,3-dia-xol-4-yl) amino)-2-deoxyglucose; FBG, fasting blood glucose; SIRT3, sirtuin 3; IR, insulin resistance; Rg1, ginsenoside Rg1; Re, ginsenoside Re; Rb1, ginsenoside Rb1; Rc, ginsenoside Rc; Rd, ginsenoside Rd; Pue, puerarin; LC-MS, liquid chromatography – mass spectrometry; STZ, streptozotocin; PA, palmitate; Pxy, puerarin 6'-O-xyloside; 3'-MP, 3'-methoxypuerarin; 4'-MP, 4'-methoxypuerarin; Dai, daidzein; Gen, genistein; Rb2, ginsenoside Rb2.

Peer review information

Traditional Medicine Research thanks Qi-Nan Wu and other anonymous reviewers for their contribution to the peer review of this paper.

Citation

Lan ZH, Tan LF, Wang GE, Tang MQ, Wang RH, Wang SM. Active compounds in RenShenJian decoction ameliorate insulin resistance in vitro. *Tradit Med Res.* 2022;7(4):32. doi: 10.53388/TMR20221022002.

Executive editor: Xiao-Ru Kou.

Received: 22 October 2021; Accepted: 06 April 2022;

Available online: 04 May 2022.

© 2022 By Author(s). Published by TMR Publishing Group Limited. This is an open access article under the CC-BY license. (<http://creativecommons.org/licenses/by/4.0/>)

Abstract

Background: RenShenJian decoction, a combination of *Pueraria lobata* (Willd.) Ohwi and *Panax ginseng* C. A. Mey, has been used in China since the Song Dynasty (960–1279 C.E.) to relieve symptoms of diabetes mellitus. However, the key compounds in RenShenJian that ameliorate insulin resistance remain unclear. This study identified the anti-diabetic compounds in RenShenJian by rescuing the decreased function of adenosine 5'-monophosphate-activated protein kinase (AMPK), sirtuin 3 (SIRT3), or glucose transporter isoform 4 (GLUT4). **Methods:** After streptozotocin-induced diabetic mice were treated with RenShenJian, fasting blood glucose levels and protein expression of SIRT3, p-AMPK, and AMPK were determined. Compounds from RenShenJian in plasma were monitored using multiple responses by liquid chromatography – mass spectrometry. Additionally, two insulin-resistant cell models were incubated with compounds identified in RenShenJian in the blood. Glucose uptake was determined using the fluorescent analog 2-(N-(7-nitrobenz-2-oxa-1,3-dia-xol-4-yl)amino)-2-deoxyglucose. Protein expression levels of p-AMPK, AMPK, SIRT3, and GLUT4 were detected by western blotting. **Results:** RenShenJian decreased FBG levels and upregulated SIRT3 expression and AMPK phosphorylation in diabetic mice. Thirteen RenShenJian extracts were identified in the blood, 11 of which increased the ratios of 2-(N-(7-nitrobenz-2-oxa-1,3-dia-xol-4-yl)amino)-2-deoxyglucose uptake in two insulin-resistant cell models. Nine extracts increased AMPK phosphorylation, nine increased SIRT3 expression, and six elevated GLUT4 expression in palmitate-induced HepG2 cells. Five extracts – puerarin, puerarin 6'-O-xyloside, genistein, ginsenoside Rb1, and ginsenoside Rd – simultaneously activated AMPK, SIRT3 and GLUT4. **Conclusion:** A series of compounds in RenShenJian that target AMPK, SIRT3, and/or GLUT4 was confirmed and indicate the chemical material basis of amelioration of insulin resistance by RenShenJian.

Keywords: SIRT3; AMPK; GLUT4; diabetes; *Pueraria lobata* (Willd.) Ohwi; *Panax ginseng* C. A. Mey

Highlights

Thirteen proto-constituents of RenShenJian in the blood of rats were identified by liquid chromatography – mass spectrometry after oral administration of RenShenJian decoction, and six were confirmed to improve insulin resistance by targeted activation of the AMPK/SIRT3/GLUT4 pathway, providing a chemical basis for the hypoglycemic effect of RenShenJian.

Medical history of objective

RenShenJian decoction was first recorded in volume 58 of *General Records of Holy Universal Relief* (compiled in 1117 C.E. by the imperial court in the period of Song emperor Huizong) and is prepared with ginseng:*Puerariae* at a 1:2 ratio. In ancient China, both ginseng and *Puerariae* were used to treat "XiaoKe" (known as diabetes). Modern medical research has shown that they can effectively ameliorate insulin resistance. Ginseng polysaccharides, ginsenosides, and polypeptide components can suppress appetite and slow islet β -cell death. *Puerariae* and its active compounds, such as puerarin, can ameliorate insulin resistance by increasing glucose transporter 4 content and enhancing insulin sensitivity in type II diabetes. However, the pharmacodynamic material basis of RenShenJian decoction compounds needs to be further explored.

Background

Type 2 diabetes mellitus is an increasingly prevalent disease and a major global public health problem. Insulin resistance (IR), the main pathogenesis of type 2 diabetes mellitus, is a manifestation of metabolic inflexibility, such as impaired inhibition of gluconeogenesis and decreased glucose disposal function in peripheral tissues, resulting in excess glucose accumulation in the blood [1].

In the liver, metabolic imbalance, such as that caused by fatty acid metabolic disorders, leads to impaired insulin sensitivity and improves compensatory insulin secretion. Excess insulin stimulation or fatty acid-induced lipotoxicity leads to IR through a decrease in glucose uptake and glucose utilization, thereby inducing ectopic fat accumulation in the liver [2, 3]. The incidence of liver-related diseases, such as nonalcoholic fatty liver disease, dyslipidemia, and metabolic syndrome, has increased. Thus, reducing fatty acids and excess insulin-induced metabolic imbalance could ameliorate IR-related liver diseases.

Palmitate, the main saturated fatty acid, induces lipotoxicity in hepatocytes and leads to IR by increasing oxidative stress [4]. Palmitate-induced endoplasmic reticulum stress is related to the expression of glucose transporters, such as glucose transporter isoform 4 (GLUT4), in HepG2 cells [5]. GLUT4 mediates extracellular glucose uptake into the cytoplasm and is regulated by the insulin signaling pathway in the liver [6]. Sirtuin 3 (SIRT3), a nicotinamide adenine dinucleotide(+) -dependent deacetylase, regulates glucose oxidation via deacetylation of key enzymes in the Krebs cycle. Reports have indicated that impaired SIRT3 activity leads to IR through activation of oxidative stress [7]. Lipotoxicity-induced IR is related to the inhibition of the energy switch adenosine 5'-monophosphate-activated protein kinase (AMPK), which disrupts the metabolic balance in peripheral tissues [8]. AMPK improves GLUT4 expression and translocation and upregulates glucose uptake [9]. Moreover, studies have indicated that AMPK activation rescues SIRT3 expression in skeletal muscle with decreased insulin sensitivity [10]. Therefore, lipotoxicity-related hepatic IR demonstrates impaired function of the AMPK/SIRT3/GLUT4 pathway. Targeting AMPK/SIRT3/GLUT4 increases insulin sensitivity.

RenShenJian (RSJ) decoction was first recorded in volume 58 of *General Records of Holy Universal Relief*, which was compiled in 1117

C.E. by the imperial court in the period of Song emperor Huizong [11]. RSJ is composed of *Panax ginseng* and *Pueraria lobata* in a 1:2 group formula and treats "XiaoKe", known as diabetes. In ancient China, ginseng and *Pueraria* were used to treat diabetes mellitus [12]. Modern medical research has shown that both can effectively improve IR [13–15]. The use of RSJ decoction has been proven in recent years to regulate metabolic disorder in diabetic rats and reduce blood glucose levels [16, 17].

Previous studies have indicated that ginseng extract reduces serum glucose levels by upregulating AMPK and GLUT4 in diabetic mice [18]. Ginseng extract also improves SIRT3 expression in aging rats [19]. *P. lobata* extract also augments AMPK activity and GLUT4 expression [20, 21]. Thus, we hypothesized that RSJ ameliorates hepatic IR via the AMPK/SIRT3/GLUT4 pathway. More than 200 and 120 components, such as ginsenoside Rg1 (Rg1), ginsenoside Re (Re), ginsenoside Rb1 (Rb1), ginsenoside Rc (Rc), ginsenoside Rd (Rd), and puerarin (Pue), have been found in *P. ginseng* and *P. lobata*, respectively; however, the chemical components of RSJ that ameliorate hepatic IR, at least via the AMPK/SIRT3/GLUT4 pathway, remain unclear [22, 23]. In this study, the active compounds of RSJ extracts that ameliorate IR were identified in the blood, and the underlying mechanism involved was deduced.

Materials and methods

Preparation of RSJ extract

P. lobata and *P. ginseng* were authenticated by Mr. Jizhu Liu from the College of Traditional Chinese Medicine, Guangdong Pharmaceutical University, and voucher specimens were deposited at the Department of Traditional Chinese Medicine Analysis, Guangdong Pharmaceutical University, with accession numbers GDPUTCM-PL2018-R01 (*P. lobata*) and GDPUTCM-PG2018-101 (*P. ginseng*).

P. lobata (240 g) and *P. ginseng* (120 g) were immersed in distilled water (1:10, w/v) for 0.5 h and then boiled for 1.5 h. After filtration, the filter residues were boiled in distilled water (1:8, w/v) for 1 h. After filtration, the filtrates were combined at a concentration of 1.5 g/mL. Protein and soluble cellulose in the extracts were removed using 70% ethanol, and the supernatant was evaporated to dryness. The dry products were dissolved in water at a concentration of 1.5 g/mL. For quantification of the main chemicals in the RSJ extract, samples were detected using a Thermo Scientific Q Exactive Focus Orbitrap liquid chromatography – mass spectrometry (LC-MS) system (Thermo Fisher Scientific, Waltham, MA, USA).

Animal experiments and treatments

Male specific pathogen-free Sprague-Dawley rats were orally administered 18.8 g/kg (the maximum tolerated dose for rats in pre-experiments) of RSJ extract twice daily for 5 days. Before the last treatment, blood samples were collected from the inner canthus, which served as a blank. At the last treatment, the rats were administered RSJ extract 1 h before being sacrificed. Blood samples were collected from the inner canthus of the eyes and used as RSJ-treated blood samples. After centrifugation (1,685 \times g, 3 min), the serum samples were collected. Each serum sample (300 μ L) was added with 1.2 mL methanol for protein precipitation, followed by centrifugation at 9,718 \times g for 20 min. The supernatant was transferred to a new tube and evaporated to dryness under nitrogen at 40 $^{\circ}$ C. After reconstitution with 60% methanol, the supernatants were filtered through 0.22- μ m filters and used for LC-MS analysis.

Male specific pathogen-free C57BL/6J mice (18–22 g) were fed a high-fat diet for 8 weeks. The remaining mice were fed a normal diet. high-fat diet fed mice were administered intraperitoneal injections of streptozotocin (STZ, 40 mg/kg) once a day for 4 consecutive days. The normal diet and high-fat diet groups were injected with the same dose of citric acid-sodium buffer. STZ-induced mice with fasting blood glucose levels > 11.1 mmol/L were randomly assigned to the STZ group. Two doses (3 and 5.43 g/kg) of RSJ were administered to the STZ-induced mice for an additional 6 weeks. On the last day, all mice were sacrificed. Plasma and liver tissue samples were also collected.

Fasting blood glucose was determined using a glucose kit and the glucose oxidase method (Nanjing Jiancheng Bioengineering Institute, Nanjing, China). Based on the results of the preliminary experiment for dilution concentration, the plasma sample was diluted 10 times with distilled water to be tested. Then, 2.5 μ L of sample was added to 250 μ L of working solution and incubated at 37 °C for 10 min after gentle shaking, and the absorbance value was determined at a wavelength of 505 nm. Blank wells were replaced with 2.5 μ L of distilled water, and standard wells were replaced with 2.5 μ L of standard. The calculation formula is as follows:

$$\text{Glucose (mmol/L)} = \frac{\text{OD}_{\text{test}} - \text{OD}_{\text{blank}}}{\text{OD}_{\text{standard}} - \text{OD}_{\text{blank}}} \times \text{standard (mmol/L)} \times \text{dilution times}$$

Sprague-Dawley rats and C57BL/6J mice were provided by the Laboratory Animal Center of Guangzhou University of Chinese Medicine and Guangdong Medical Laboratory Animal Center (Guangdong, China), respectively. All animal experimental procedures were approved by the Animal Ethics Committee of Guangdong Pharmaceutical University (approval number: SYXK (Yue) 2017-0125).

LC-MS analysis

LC separations were performed on a Dionex Ultimate UPLC 3000 system (Thermo Fisher Scientific, Waltham, MA, USA) with an ACQUITY UPLC® BEH C18 column (1.7 μ m, 2.1 \times 100 mm, Waters Corp., Milford, MA, USA). The analysis was performed within 44 min at a flow rate of 0.3 mL/min. Samples were eluted using a gradient of 0.1% (v/v) formic acid (solvent A) and acetonitrile (solvent B) as follows: 0–5 min, 5%–19% (B); 5–14 min, 19%–22% (B); 14–35 min, 22%–40% (B); 35–38 min, 40%–90% (B); 38–40 min, 90% (B); 40–41 min, 90%–19% (B); and 41–44 min, 19%–5% (B). The mass spectrometer was operated in negative electrospray ionization full MS-dd-MS/MS acquisition mode with the following parameter settings: sheath flow rate, 45; assistant flow rate, 10 AU; spray voltage, 3 KV; assistant temperature, 200 °C; and capillary temperature, 320 °C. Full scan data were recorded for ions with m/z 100–1,500 (Supplementary Figure S1 and Supplementary Tables S1 and S2). The quantification of the RSJ compounds was confirmed by comparison with the MS data (mzCloud: <https://www.mzcloud.org/>, mzVault, ChemSpider: <http://www.chemspider.com/>) and retention times of Pue, Rg1, Re, and Rb1 standards.

Cell culture and treatments

Human hepatocellular carcinoma cell line HepG2 cells (purchased from the cell bank of the Chinese Academy of Sciences) was cultured in Dulbecco's modified Eagle medium supplemented with 10% fetal bovine serum and 1% penicillin and streptomycin in the presence of 5% CO₂ at 37 °C. HepG2 cells were incubated in serum-free low-glucose Dulbecco's modified Eagle medium for 12 h, then stimulated with 100 nM insulin (Macklin, Shanghai, China) or 0.2 mM palmitate (PA, Sigma, St. Louis, MO, USA) for 24 h to establish insulin-resistant hepatocyte models [24, 25]. Appropriate concentrations of Pue, puerarin 6'-O-xyloside (Pxy), 3'-methoxypuerarin (3'-MP), 4'-methoxypuerarin (4'-MP), Rg1, daidzein (Dai), genistein (Gen), Rb1, ginsenoside Rb2 (Rb2), Rc, and Rd (Chroma-Biotechnology, Chengdu, China) were added to the two insulin-resistant hepatocyte models for 24 h. The purity of all compounds was higher than 98%.

2-(N-(7-nitrobenz-2-oxa-1,3-dia-xol-4-yl)amino)-2-deoxyglucose (2-NBDG) uptake assay

Glucose uptake was determined using the glucose fluorescent analog 2-NBDG (Invitrogen, Barcelona, Spain). Briefly, HepG2 cells were incubated with 50 μ M 2-NBDG for 30 min. Subsequently, cells were washed twice with phosphate-buffered saline. Fluorescence intensity was immediately measured at an excitation wavelength of 485 nm and emission wavelength of 535 nm [26]. The 2-NBDG content was quantified based on fluorescence intensity. Ratios of 2-NBDG uptake were calculated by normalization to the insulin or PA group.

Western blot analysis

Liver tissues and cells were homogenized using radioimmunoprecipitation assay lysis buffer (Beyotime Biotechnology, Shanghai, China). After centrifugation at 12,000 rpm for 15 min, the supernatants were collected. After quantitation, the protein lysates were separated by sodium dodecyl sulfate-polyacrylamide gel electrophoresis and transferred to polyvinylidene difluoride membranes (Merck KGaA, Germany). Subsequently, the membranes were blocked with 5% nonfat milk for 2 h, followed by incubation overnight at 4 °C with primary antibodies, including AMPK (1:1000, Cell Signaling Technology, Boston, MA, USA), phospho-AMPK (1:1000, Cell Signaling Technology), SIRT3 (1:1000, Cell Signaling Technology), GLUT4 (1:500, Proteintech, Chicago, IL, USA), and glyceraldehyde-3-phosphate dehydrogenase (1:500, Proteintech). Membranes were incubated with horseradish peroxidase-conjugated goat anti-rabbit secondary antibody (1:6000, Proteintech) for 2 h at room temperature. The blotted membrane was detected by enhanced chemiluminescence using ECL Western blotting detection substrate (Thermo Scientific, Waltham, MA, USA).

Statistical analysis

Data are expressed as mean \pm standard deviation and were analyzed using one-way ANOVA in SPSS v.19.0 (IBM Corp., Armonk, NY, USA). $P < 0.05$ was set as a threshold of statistical significance.

Results

RSJ reduced plasma glucose and increased hepatic SIRT3 expression and AMPK phosphorylation in STZ-induced diabetic rats

To investigate the positive effects of RSJ on diabetes, STZ-induced diabetic rats demonstrating high plasma glucose levels were administered two doses of RSJ. The two doses significantly decreased plasma glucose levels compared with those in the STZ group ($P < 0.01$, Figure 1A) and had effects comparable with those of 200 mg/kg metformin. As shown in Figure 1B, SIRT3 expression and AMPK phosphorylation in the liver were reduced in the STZ-induced mice. AMPK phosphorylation and SIRT3 expression increased in diabetic mice administered 5.34 g/kg RSJ ($P < 0.01$ and $P < 0.05$, respectively).

Thirteen major compounds in RSJ in the blood were identified

For further investigation, we detected the compounds in RSJ in the blood of rats treated with RSJ using LC-MS. As shown in Figure 2 and Table 1, 13 compounds Pue, Dai, 3'-MP, 4'-MP, Pxy, mirificin, formononetin, Gen, Rg1, Rb1, Rb2, Rc, and Rd were identified based on structural confirmation, retention time, and the m/z values of the molecular ions.

The primary MS data of peak 2 indicated that m/z 547.15948 was $[\text{M-H}]^-$, and the molecular formula predicted by Thermo Xcalibur 3.0 software was C₂₆H₂₈O₁₃. Secondary MS analysis was performed using m/z 547.15948 as the parent ion, and the secondary ion fragments obtained were 547.15948 $[\text{M-H}]^- \rightarrow 295[\text{M-H-xy-C}_4\text{H}_8\text{O}_4]^- \rightarrow 267[\text{M-H-xy-C}_4\text{H}_8\text{O}_4\text{-CO}]^-$. Based on data from a previous report, peak 2 was characterized as Pxy. Similarly, for peak 3, the molecular formula was determined to be C₂₂H₂₂O₁₀ [27]. The secondary ion fragments obtained were 445.11368 $[\text{M-H}]^- \rightarrow 325[\text{M-H-C}_4\text{H}_8\text{O}_4]^- \rightarrow 282[\text{M-H-163}]^-$. For peak 5, the molecular formula was C₂₂H₂₂O₉, and the secondary ion fragments obtained were 429.08228 $[\text{M-H}]^- \rightarrow 309[\text{M-H-C}_4\text{H}_8\text{O}_4]^- \rightarrow 266[\text{M-H-163}]^-$. For peak 10, the molecular formula was C₅₃H₉₀O₂₂, and the secondary ion fragments obtained were 1123.59082 $[\text{M}+\text{HCOO}]^- \rightarrow 783[\text{M-H-132-gluc}]^- \rightarrow 621[\text{M-H-132-2gluc}]^-$. For peak 13, the molecular formula was C₁₆H₁₂O₄, and the secondary ion fragments obtained were 267.06607 $[\text{M-H}]^- \rightarrow 252[\text{M-H-CH}_3]^- \rightarrow 223[\text{M-H-CO}_2]^-$.

According to the characteristic fragmentations of compounds described in references, peaks 3, 5, 10, and 13 were characterized as 3'-MP, 4'-MP, Rb2, and formononetin [23, 27]. Peaks 4 and 2 were two isomers, and peak 4 was determined according to the retention

time to be mirificin. Peaks 1, 6, 7, 8, 9, 11, and 12 were identified using MS data (supplementary results) and retention time.

Eleven compounds in RSJ in the blood increased 2-NBDG uptake in insulin-resistant HepG2 cells

To investigate whether the 13 main plasma compounds in RSJ ameliorate IR, the glucose uptake activities of the compounds were determined using insulin- or palmitate-induced insulin-resistant HepG2 cells. These HepG2 cells demonstrated decreased ratios of 2-NBDG uptake compared with that in the control group. Eleven compounds Pue, 3'-MP, Pxy, Dai, 4'-MP, Gen, Rg1, Rb1, Rb2, Rc, and Rd significantly increased 2-NBDG uptake in insulin-induced insulin-resistant HepG2 cells (Figure 3A) and palmitate-induced insulin-resistant HepG2 cells (Figure 3B). The results indicated that these components contributed to the positive effects of RSJ on

relieving hepatic IR.

Glucose uptake activators from RSJ targeted AMPK, SIRT3, or GLUT4 in insulin-resistant HepG2 cells

Next, we investigated whether the 11 compounds activated AMPK, SIRT3, or their downstream regulator, GLUT4, in insulin-resistant cells. As shown in Figure 4A and B, Pue, 3'-MP, Pxy, 4'-MP, Gen, Rb1, Rb2, Rc, and Rd significantly increased AMPK phosphorylation in palmitate-induced insulin-resistant HepG2 cells ($P < 0.05$, $P < 0.01$). Nine of the eleven compounds Pue, 3'-MP, Pxy, Dai, 4'-MP, Gen, Rb1, Rd, and Rg1 increased SIRT3 expression ($P < 0.05$, $P < 0.01$). In addition, GLUT4 expression in insulin-resistant HepG2 cells was improved by incubation with Pue, Pxy, Gen, Rb1, Rd, and Rg1 ($P < 0.05$, $P < 0.01$). Five of these Pue, Pxy, Gen, Rb1, and Rd activated AMPK, SIRT3, and GLUT4 simultaneously.

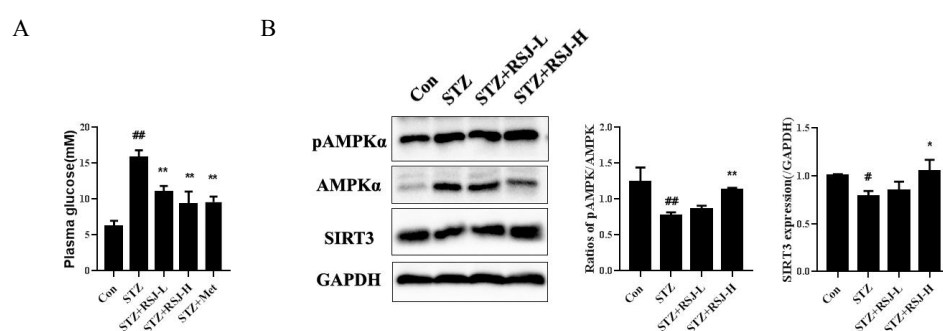


Figure 1 RenShenJian reduced fasting blood glucose levels and increased hepatic SIRT3 expression and AMPK phosphorylation in STZ-induced diabetic mice. STZ-induced diabetic mice were treated with two doses of RSJ daily for 6 weeks. (A) Plasma glucose levels were measured. (B) SIRT3 expression and AMPK phosphorylation were determined using western blotting. Data were collected from 6 mice in each group. Significant differences were observed relative to the control group at $^{\#}P < 0.05$ and $^{##}P < 0.01$ and to the STZ-treated group at $*P < 0.05$, and $**P < 0.01$. Con, control group; STZ, streptozotocin-treated group; STZ + RSJ-L, STZ-induced mice administered 3 g/kg RSJ; STZ + RSJ-H, STZ-induced mice administered 5.43 g/kg RSJ; STZ + Met, STZ-induced mice administered 200 mg/kg metformin. RSJ, RenShenJian; AMPK, adenosine 5'-monophosphate-activated protein kinase; SIRT3, sirtuin 3; STZ, streptozotocin; GAPDH, glyceraldehyde-3-phosphate dehydrogenase.

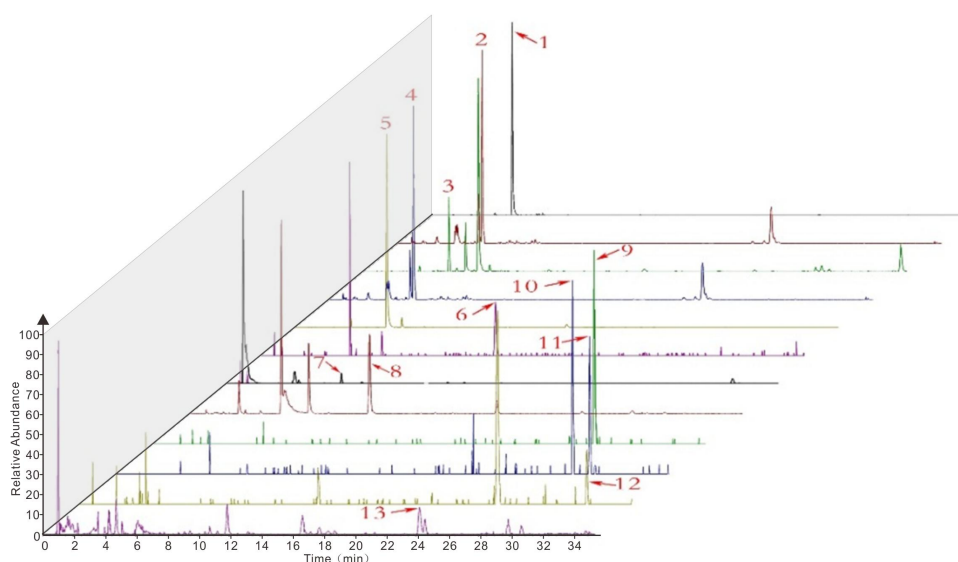


Figure 2 Thirteen major compounds in RSJ in the blood after rats treated with RSJ were identified. Blood samples were collected 1 h after RSJ administration. Blood samples were disposed of and analyzed using LC-MS/MS in negative mode. Data acquisition and total ion chromatograms were processed using Thermo Xcalibur 3.0. The X-axis represents retention time, and the Y-axis represents relative abundance. According to the product spectra and fragmentation patterns of the analytes, the numbers from the figure above represent the following compounds in RSJ: 1, Pue; 2, Pxy; 3, 3'-MP; 4, mirificin; 5, 4'-MP; 6, Rg1; 7, Dai; 8, Gen; 9, Rb1; 10, Rb2; 11, Rc; 12, Rd; 13, formononetin. RSJ, RenShenJian; Rg1, ginsenoside Rg1; Re, ginsenoside Re; Rb1, ginsenoside Rb1; Rc, ginsenoside Rc; Rd, ginsenoside Rd; Pue, puerarin; LC-MS, liquid chromatography – mass spectrometry; Pxy, puerarin 6'-O-xyloside; 3'-MP, 3'-methoxypuerarin; 4'-MP, 4'-methoxypuerarin; Dai, daidzein; Gen, genistein; Rb2, ginsenoside Rb2.

Table 1 Chemical data of the ingredients of RSJ in the blood and their concentrations

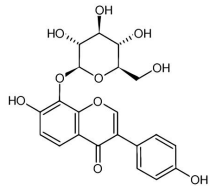
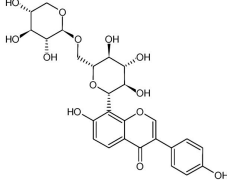
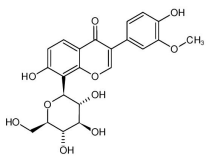
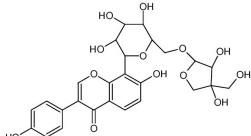
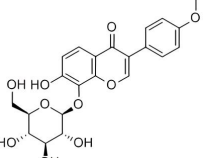
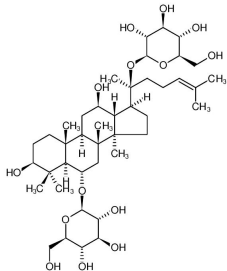
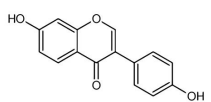
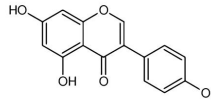
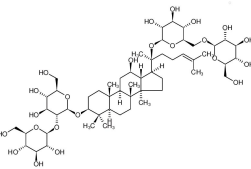
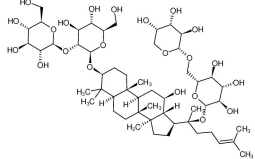
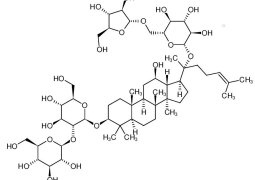
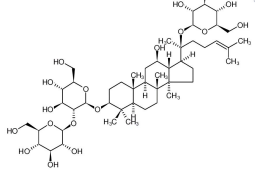
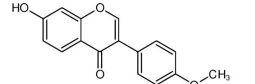
No.	Compound	Retention time/min	MS ¹ (m/z)	Mass error/ppm	Molecular formula	Fragmentation (m/z)	Concentrations (nM)	Chemical structure
1	Pue	5.12	415.10297 [M-H] ⁻	1.473	C ₂₁ H ₂₀ O ₉	415, 295, 267	33.70	
2	Pxy	5.40	547.15948 [M-H] ⁻	1.175	C ₂₆ H ₂₈ O ₁₃	295, 267	Not quantified	
3	3'-MP	5.47	445.11368 [M-H] ⁻	1.700	C ₂₂ H ₂₂ O ₁₀	445, 325, 282	Not quantified	
4	Mir	5.42	547.14532 [M-H] ⁻	1.284	C ₂₆ H ₂₈ O ₁₃	295, 267	Not quantified	
5	4'-MP	5.89	429.08228 [M-H] ⁻	1.228	C ₂₂ H ₂₂ O ₉	429, 309, 266, 253	Not quantified	
6	Rg1	15.07	845.48993 [M + HCOO] ⁻	0.730	C ₄₂ H ₇₂ O ₁₄	845, 799	0.16	
7	Dai	11.56	253.05013 [M-H] ⁻	2.350	C ₁₅ H ₁₀ O ₄	253, 225, 209	2.60	
8	Gen	7.36	269.04517 [M-H] ⁻	1.859	C ₁₅ H ₁₀ O ₅	269, 241, 225	4.74	
9	Rb1	28.34	1153.60071 [M + HCOO] ⁻	0.577	C ₅₄ H ₉₂ O ₂₃	1107, 945, 783, 621	0.88	

Table 1 Chemical data of the ingredients of RSJ in the blood and their concentrations (Continued)

No.	Compound	Retention time/min	MS ¹ (<i>m/z</i>)	Mass error/ ppm	Molecular formula	Fragmentation (<i>m/z</i>)	Concentrations (nM)	Chemical structure
10	Rb2	29.30	1123.59045 [M + HCOO] ⁻	0.864	C ₅₃ H ₉₀ O ₂₂	1077, 945, 783, 621	Not quantified	
11	Rc	30.39	1123.59082 [M + HCOO] ⁻	1.193	C ₅₃ H ₉₀ O ₂₂	1077, 945, 783, 621	0.43	
12	Rd	32.60	991.54913 [M + HCOO] ⁻	1.925	C ₄₈ H ₈₂ O ₁₈	945, 783, 621, 459	0.11	
13	Form	24.23	267.06607 [M-H] ⁻	3.313	C ₁₆ H ₁₂ O ₄	267, 252, 223	Not quantified	

Mir, mirificin; Form, formononetin; RSJ, RenShenJian; Rg1, ginsenoside Rg1; Re, ginsenoside Re; Rb1, ginsenoside Rb1; Rc, ginsenoside Rc; Rd, ginsenoside Rd; Pue, puerarin; Pxy, puerarin 6'-O-xyloside; 3'-MP, 3'-methoxypuerarin; 4'-MP, 4'-methoxypuerarin; Dai, daidzein; Gen, genistein; Rb2, ginsenoside Rb2.

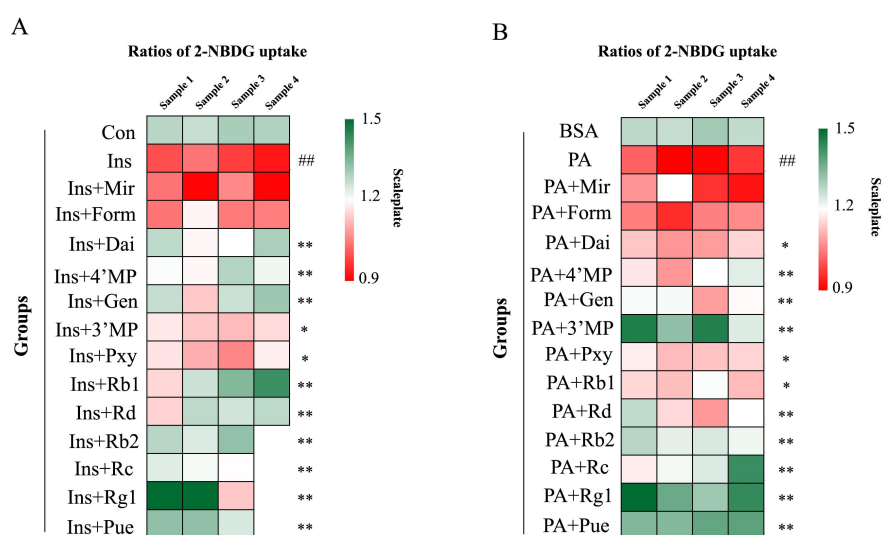


Figure 3 Thirteen compounds in RenShenJian in the blood increased 2-NBDG uptake in insulin-resistant HepG2 cells. Insulin-resistant HepG2 cells were treated with insulin or palmitate for 24 h. (A) Compounds in RSJ were administered to insulin-induced HepG2 cells for 24 h. (B) Compounds in RSJ were administered to palmitate-induced HepG2 cells for 24 h. Heat maps indicate the ratios of 2-NBDG uptake in different groups. The relative ratio of 2-NBDG uptake in each group was normalized to that in the Ins or PA group. Red indicates downregulation, whereas green indicates upregulation. Data were collected from 3 or 4 samples from each group. Significant differences were observed relative to the control or bovine serum albumin (BSA) group at ^{##}*P* < 0.01 and to the Ins or PA group at **P* < 0.05 and ***P* < 0.01. Control and BSA, control groups; Ins, insulin-induced insulin-resistant HepG2 cells; PA, palmitate-induced insulin-resistant HepG2 cells; Ins + Pue et al., insulin-induced cells treated with the different compounds; PA + Pue et al., palmitate-induced cells treated with the different compounds. 2-NBDG, 2-(N-(7-nitrobenz-2-oxa-1,3-dia-xol-4-yl) amino)-2- deoxyglucose; RSJ, RenShenJian; Mir, mirificin; Form, formononetin; Rg1, ginsenoside Rg1; Re, ginsenoside Re; Rb1, ginsenoside Rb1; Rc, ginsenoside Rc; Rd, ginsenoside Rd; Pue, puerarin; Pxy, puerarin 6'-O-xyloside; 3'-MP, 3'-methoxypuerarin; 4'-MP, 4'-methoxypuerarin; Dai, daidzein; Gen, genistein; Rb2, ginsenoside Rb2.

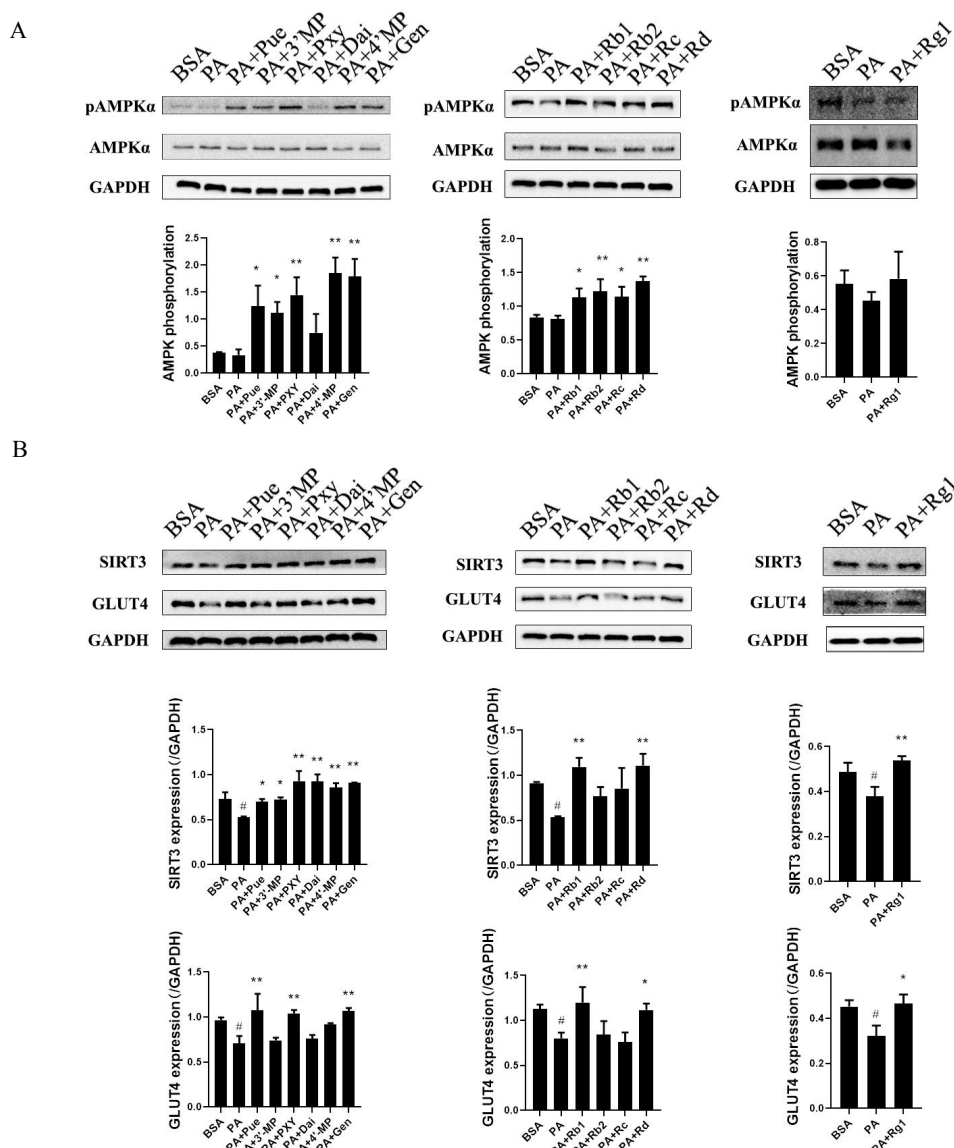


Figure 4 Glucose uptake activators from RSJ targeted AMPK, SIRT3, or GLUT4 in insulin-resistant HepG2 cells. Palmitate-induced insulin-resistant HepG2 cells were incubated with glucose uptake activators from RSJ for 24 h. (A) Phosphorylation of AMPK and (B) expression of SIRT3 and GLUT4 were determined by western blotting. Data were collected from three samples in each group. Significant differences were observed relative to the BSA group at $^{\#}P < 0.05$ and $^{\#}P < 0.01$ and to the PA group at $*P < 0.05$ and $**P < 0.01$. BSA, control group; PA, palmitate-induced insulin-resistant HepG2 cells; PA + Pue et al., palmitate-induced cells treated with the different compounds. GLUT4, glucose transporter isoform 4; AMPK, adenosine 5'-monophosphate-activated protein kinase; 2-NBDG, 2-(N-(7-nitrobenz-2-oxa-1,3-dia-xol-4-yl) amino)-2-deoxyglucose; SIRT3, sirtuin 3; GAPDH, glyceraldehyde-3-phosphate dehydrogenase; RSJ, RenShenJian; Mir, mirificin; Form, formononetin; Rg1, ginsenoside Rg1; Re, ginsenoside Re; Rb1, ginsenoside Rb1; Rc, ginsenoside Rc; Rd, ginsenoside Rd; Pue, puerarin; Pxy, puerarin 6'-O-xyloside; 3'-MP, 3'-methoxypuerarin; 4'-MP, 4'-methoxypuerarin; Dai, daidzein; Gen, genistein; Rb2, ginsenoside Rb2.

Discussion

RSJ demonstrated anti-diabetic effects in the clinic and in STZ-induced diabetic mice, and the chemical basis and mechanism of RSJ in ameliorating hepatic IR were investigated. According to the pharmacokinetics of active compounds from ginseng and *Pueraria*, components such as Pue, Dai, Rg1, Re, Rb1, Rc, and Rd can be absorbed into the blood with different pharmacokinetic parameters in rats and mice, but there are few differences in biotransformation pathways [27–29]. Thirteen proto-constituents of RSJ Pue, 3'-MP, Pxy, Dai, 4'-MP, Gen, Rg1, Rb1, Rb2, Rc, Rd, formononetin, and mirificin were identified in the blood after RSJ administration.

Hepatic IR causes various diabetes-related complications, such as nonalcoholic fatty liver disease, dyslipidemia, and metabolic

syndrome. Our study found that chemicals such as Pue, 3'-MP, Pxy, Dai, 4'-MP, Gen, Rg1, Rb1, Rb2, Rc, and Rd reversed the reduction in glucose utilization in the liver. Our data confirmed the antidiabetic basis of RSJ.

As a traditional Chinese medicine, RSJ is characterized by multiple components, targets, and pathways. Previous data have demonstrated that compound K in ginseng can improve insulin sensitivity by regulating the PI3K/Akt signaling pathway to achieve a hypoglycemic effect [30]. Re alleviates IR by activating the peroxisome proliferator-activated receptors- γ pathway, upregulating peroxisome proliferator-activated receptors- γ 2, promoting GLUT4 translocation, and increasing glucose uptake [31]. Pue can regulate the I κ B kinase beta/insulin receptor substrates signaling pathway to inhibit inflammation and alleviate endothelial IR [32].

The present data indicate that Pue, Pxy, Gen, Rb1, and Rd from RSJ regulate AMPK/SIRT3/GLUT4 activation in insulin-resistant hepatocytes. Some traditional Chinese medicines relieve symptoms of polydipsia, polyuria, and marasmus via activation of the AMPK/SIRT3/GLUT4 pathway [33, 34]. Therefore, upregulation of AMPK/SIRT3/GLUT4 function might be a potential mechanism by which RSJ ameliorates IR. Impaired SIRT3 activity leads to IR through increased reactive oxygen species production and inhibition of β -oxidation [7]. SIRT3 activators of RSJ may improve energy metabolism in hepatocytes, thereby increasing glucose metabolic flux.

Several mechanisms underlying the hypoglycemic effects of ginseng and *Pueraria* were also proposed in the current study, including inhibition by ginseng of cytokine-induced apoptosis of pancreatic insulin-producing β -cells. Several components of RSJ extracts in blood, such as Pue, Gen, Rg1, Rb1, and Rd, have been used to treat diabetic or nonalcoholic fatty liver disease through AMPK-related signaling pathways [35–40]. Our data also showed that 3'-MP, Pxy, 4'-MP, Rb2, and Rc activate AMPK phosphorylation.

In conclusion, six active compounds that alleviate IR were confirmed, which indicated the chemical material basis of RSJ increasing insulin sensitivity (Figure 5). These components exert a synergistic effect by targeting AMPK/SIRT3/GLUT4. The component group Pue, 3'-MP, Pxy, Dai, 4'-MP, Gen, Rg1, Rb1, Rb2, Rc, and Rd partly explains the mechanism of the anti-diabetic effects of RSJ.

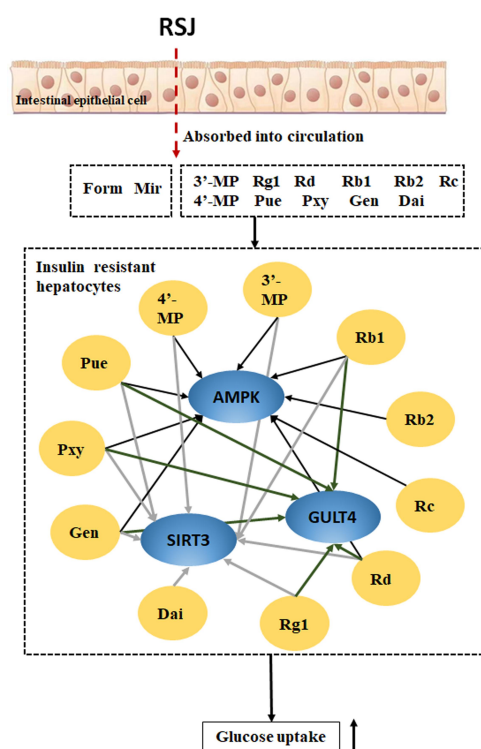


Figure 5 Eleven glucose uptake activators from RSJ confirmed the probable basis of IR amelioration by RSJ partly by upregulation of AMPK/SIRT3/GLUT4 function. GLUT4, glucose transporter isoform 4; AMPK, adenosine 5'-monophosphate-activated protein kinase; RSJ, RenShenJian; SIRT3, sirtuin 3; 3'-MP, 3'-methoxypuerarin; Rg1, ginsenoside Rg1; Rd, ginsenoside Rd; Rb1, ginsenoside Rb1; Rb2, ginsenoside Rb2; Rc, ginsenoside Rc; 4'-MP, 4'-methoxypuerarin; Pue, puerarin; Pxy, puerarin 6'-O-xyloside; Gen, genistein; Dai, daidzein.

Chemical data of the RSJ compounds in the blood and their concentrations were determined by LC-MS/MS analysis. Compounds 1, 6, 7, 8, 9, 11, and 12 were identified using standard substances, Pue, Rg1, Dai, Gen, Rb1, Rc, and Rd, based on their product spectra and fragmentation patterns. Compounds 2, 3, 4, 5, 10, and 13 were

identified by analyzing their secondary cleavage rules and comparing them with data from previous research [17, 22, 23]. The concentrations of Pue, Dai, Gen, Rg1, Rb1, Rc, and Rd in the blood were calculated using external standards as quantitative methods.

References

- Kalra S, Unnikrishnan AG, Baruah MP, Sahay R, Bantwal G. Metabolic and energy imbalance in dysglycemia-based chronic disease. *Diabetes Metab Syndr Obes.* 2021;14:165–184. <https://doi.org/10.2147/DMSO.S286888>
- Jiang CJ, Zhang SS, Li D, et al. Impaired ferritinophagy flux induced by high fat diet mediates hepatic insulin resistance via endoplasmic reticulum stress. *Food Chem Toxicol.* 2020;140:111329. <https://doi.org/10.1016/j.fct.2020.111329>
- Yang XF, Mei S, Gu HH, et al. Exposure to excess insulin (glargine) induces type 2 diabetes mellitus in mice fed on a chow diet. *J Endocrinol.* 2014;221(3):469–480. <https://doi.org/10.1530/JOE-14-0117>
- Galmés-Pascual BM, Martínez-Cignoni MR, Morán-Costoya A, et al. 17 β -Estradiol ameliorates lipotoxicity-induced hepatic mitochondrial oxidative stress and insulin resistance. *Free Radic Biol Med.* 2020;150:148–160. <https://doi.org/10.1016/j.freeradbiomed.2020.02.016>
- Zhang Y, Yan LS, Ding Y, et al. *Edgeworthia gardneri* (Wall.) Meisn. water extract ameliorates palmitate induced insulin resistance by regulating IRS1/GSK3 β /FoxO1 signaling pathway in human HepG2 hepatocytes. *Front Pharmacol.* 2020;10:1666. <https://doi.org/10.3389/fphar.2019.01666>
- Vazirani RP, Verma A, Sadacca LA, et al. Disruption of adipose Rab10-dependent insulin signaling causes hepatic insulin resistance. *Diabetes.* 2016;65(6):1577–1589. <https://doi.org/10.2337/db15-1128>
- Cortés-Rojas C, Vargas-Vargas MA, Olmos-Orizaba BE, Rodríguez-Orozco AR, Calderón-Cortés E. Interplay between NADH oxidation by complex I, glutathione redox state and sirtuin-3, and its role in the development of insulin resistance. *Biochim Biophys Acta Mol Basis Dis.* 2020;1866(8):165801. <https://doi.org/10.1016/j.bbadis.2020.165801>
- Kwak HJ, Choi HE, Cheon HG. 5-LO inhibition ameliorates palmitic acid-induced ER stress, oxidative stress and insulin resistance via AMPK activation in murine myotubes. *Sci Rep.* 2017;7(1):5025. <https://doi.org/10.1038/s41598-017-05346-5>
- Li S, Huang Q, Zhang LW, et al. Effect of CAPE-pNO2 against type 2 diabetes mellitus via the AMPK/GLUT4/GSK3 β /PPAR α pathway in HFD/STZ-induced diabetic mice. *Eur J Pharmacol.* 2019;853:1–10. <https://doi.org/10.1016/j.ejphar.2019.03.027>
- Shi LY, Zhang T, Zhou Y, et al. Dihydromyricetin improves skeletal muscle insulin sensitivity by inducing autophagy via the AMPK-PGC-1 α -Sirt3 signaling pathway. *Endocrine.* 2015;50(2):378–389. <https://doi.org/10.1007/s12020-015-0599-5>
- Zhao J. *General Records of Holy Universal Relief*. Vol 58. Beijing: People's Medical Publishing House;2013. (Chinese) ISBN:978-7-117-16562-4
- Zhao L, Mu YN, Liang MX. Comparison of application rules of Chinese herbal medicines on wastingthirst disease in ancient and present China. *J Beijing Univ Tradit Chin Med.* 2016;39(9):769–773. (Chinese) <https://doi.org/10.3969/j.issn.1006-2157.2016.09.014>
- Xie JT, Mchendale S, Yuan CS. Ginseng and diabetes. *Am J Chin Med.* 2005;33(3):397–404. <https://doi.org/10.1142/S0192415X05003004>
- Karmazyn M, Gan XT. Ginseng for the treatment of diabetes and diabetes-related cardiovascular complications: a discussion of the evidence. *Can J Physiol Pharmacol.* 2019;97(4):265–276.

- <https://doi.org/10.1139/cjpp-2018-0440>
15. Wong KH, Li GQ, Li KM, Razmovski-Naumovski V, Chan K. Kudzu root: traditional uses and potential medicinal benefits in diabetes and cardiovascular diseases. *J Ethnopharmacol*. 2011;134(3):584–607.
<https://doi.org/10.1016/j.jep.2011.02.001>
 16. Yu HZ, Lin WD, Wang SM. Effect of Ginseng recipe on blood glucose and serum lipoprotein metabolism in type 2 diabetes rats. *Guangdong Chem Ind*. 2017;44(2):20–21 + 40. (Chinese)
<https://doi.org/10.3969/j.issn.1007-1865.2017.02.009>
 17. Zheng HT, Li KN, Chen C, Lin WD, Wang SM. Effects of Renshenjian decoction on pancreatic metabonomic profiles in insulin resistance rats based on H-NMR metabonomics. *China J Chin Mater Medica*. 2018;43(14):3012–3017. (Chinese)
<https://doi.org/10.19540/j.cnki.cjcmm.20180327.003>
 18. Kang OH, Shon MY, Kong R, et al. Anti-diabetic effect of black ginseng extract by augmentation of AMPK protein activity and upregulation of GLUT2 and GLUT4 expression in db/db mice. *BMC Complement Altern Med*. 2017;17(1):341.
<https://doi.org/10.1186/s12906-017-1839-4>
 19. Luo P, Dong GT, Liu L, Zhou H. The long-term consumption of ginseng extract reduces the susceptibility of intermediate-aged hearts to acute ischemia reperfusion injury. *PLoS One*. 2015;10(12):e0144733.
<https://doi.org/10.1371/journal.pone.0144733>
 20. Jung HW, Kang AN, Kang SY, Park YK, Song MY. The root extract of *Pueraria lobata* and its main compound, puerarin, prevent obesity by increasing the energy metabolism in skeletal muscle. *Nutrients*. 2017;9(1):33.
<https://doi.org/10.3390/nu9010033>
 21. Lertpatipanpong P, Janpajit S, Park EY, Kim CT, Baek SJ. Potential anti-diabetic activity of *Pueraria lobata* flower (*Flos Puerariae*) extracts. *Molecules*. 2020;25(17):3970.
<https://doi.org/10.3390/molecules25173970>
 22. Yuan HD, Kim JT, Kim SH, Chung SH. Ginseng and diabetes: the evidences from in vitro, animal and human studies. *J Ginseng Res*. 2012;36(1):27–39.
<https://doi.org/10.5142/jgr.2012.36.1.27>
 23. Song W, Li YJ, Qiao X, Qian Y, Ye M. Chemistry of the Chinese herbal medicine *Puerariae Radix* (Ge-Gen): a review. *J Chin Pharm Sci*. 2014;23(6):347–360.
<https://doi.org/10.5246/jcps.2014.06.048>
http://en.cnki.com.cn/Article_en/CJFDTOTAL-XYGZ201406002.htm
 24. Xu LN, Yin LH, Jin Y, et al. Effect and possible mechanisms of dioscin on ameliorating metabolic glycolipid metabolic disorder in type-2-diabetes. *Phytomedicine*. 2020;67:153139.
<https://doi.org/10.1016/j.phymed.2019.153139>
 25. Chen L, Tang ZQ, Wang XH, Ma H, Shan DD, Cui SW. PKM2 aggravates palmitate-induced insulin resistance in HepG2 cells via STAT3 pathway. *Biochem Biophys Res Commun*. 2017;492(1):109–115.
<https://doi.org/10.1016/j.bbrc.2017.08.025>
 26. Cordero-Herrera I, Martín MÁ, Goya L, Ramos S. Cocoa flavonoids attenuate high glucose-induced insulin signalling blockade and modulate glucose uptake and production in human HepG2 cells. *Food Chem Toxicol*. 2014;64:10–19.
<https://doi.org/10.1016/j.fct.2013.11.014>
 27. Xu XY, Zheng YM, Fu SQ, Ran CQ. Determination of puerarin and pharmacokinetic in mouse plasma. *Lishizhen Med Mater Medica Res*. 2007;18(12):2960–2961. (Chinese)
<https://doi.org/10.3969/j.issn.1008-0805.2007.12.045>
 28. Dong WW, Han XZ, Zhao JH, et al. Metabolite profiling of ginsenosides in rat plasma, urine and feces by LC-MS/MS and its application to a pharmacokinetic study after oral administration of *Panax ginseng* extract. *Biomed Chromatogr*. 2018;32(3):e4105.
<https://doi.org/10.1002/bmc.4105>
 29. Zou T, Gu LW. TPGS emulsified zein nanoparticles enhanced oral bioavailability of daidzin: in vitro characteristics and in vivo performance. *Mol Pharm*. 2013;10(5):2062–2070.
<https://doi.org/10.1021/mp400086n>
 30. Jiang S, Ren DY, Li JR, et al. Effects of compound K on hyperglycemia and insulin resistance in rats with type 2 diabetes mellitus. *Fitoterapia*. 2014;95:58–64.
<https://doi.org/10.1016/j.fitote.2014.02.017>
 31. Gao Y, Yang MF, Su YP, et al. Ginsenoside Re reduces insulin resistance through activation of PPAR- γ pathway and inhibition of TNF- α production. *J Ethnopharmacol*. 2013;147(2):509–516.
<https://doi.org/10.1016/j.jep.2013.03.057>
 32. Huang F, Liu K, Du H, Kou JP, Liu BL. Puerarin attenuates endothelial insulin resistance through inhibition of inflammatory response in an IKK β /IRS-1-dependent manner. *Biochimie*. 2012;94(5):1143–1150.
<https://doi.org/10.1016/j.biochi.2012.01.018>
 33. Zhen Z, Chang B, Li M, et al. Anti-diabetic effects of a *Coptis chinensis* containing new traditional Chinese medicine formula in type 2 diabetic rats. *Am J Chin Med*. 2011;39(1):53–63.
<https://doi.org/10.1142/S0192415X11008646>
 34. Lin CH, Kuo YH, Shih CC. Effects of Bofu-Tsusho-San on diabetes and hyperlipidemia associated with AMP-activated protein kinase and glucose transporter 4 in high-fat-fed mice. *Int J Mol Sci*. 2014;15(11):20022–20044.
<https://doi.org/10.3390/ijms151120022>
 35. Zheng PY, Ji G, Ma ZS, et al. Therapeutic effect of puerarin on non-alcoholic rat fatty liver by improving leptin signal transduction through JAK2/STAT3 pathways. *Am J Chin Med*. 2009;37(1):69–83.
<https://doi.org/10.1142/S0192415X09006692>
 36. Hou BY, Zhao YR, Ma P, et al. Hypoglycemic activity of puerarin through modulation of oxidative stress and mitochondrial function via AMPK. *Chin J Nat Med*. 2020;18(11):818–826.
[https://doi.org/10.1016/S1875-5364\(20\)60022-X](https://doi.org/10.1016/S1875-5364(20)60022-X)
 37. Guevara-Cruz M, Godinez-Salas ET, Sanchez-Tapia M, et al. Genistein stimulates insulin sensitivity through gut microbiota reshaping and skeletal muscle AMPK activation in obese subjects. *BMJ Open Diabetes Res Care*. 2020;8(1):e000948.
<https://doi.org/10.1136/bmjdr-2019-000948>
 38. Gu DS, Yi HA, Jiang KR, et al. Transcriptome analysis reveals the efficacy of ginsenoside-Rg1 in the treatment of nonalcoholic fatty liver disease. *Life Sci*. 2021;267:118986.
<https://doi.org/10.1016/j.lfs.2020.118986>
 39. Shen L, Haas M, Wang DQH, et al. Ginsenoside Rb1 increases insulin sensitivity by activating AMP-activated protein kinase in male rats. *Physiol Rep*. 2015;3(9):e12543.
<https://doi.org/10.14814/phy2.12543>
 40. Bai LT, Gao JL, Wei F, Zhao J, Wang DW, Wei JP. Therapeutic potential of ginsenosides as an adjuvant treatment for diabetes. *Front Pharmacol*. 2018;9:423.
<https://doi.org/10.3389/fphar.2018.00423>